The Astrophysical Journal, 686:1372–1382, 2008 October 20

THE CURRENT SHEET ASSOCIATED WITH THE 2003 NOVEMBER 4 CORONAL MASS EJECTION: DENSITY, TEMPERATURE, THICKNESS, AND LINE WIDTH

A. Ciaravella[1,2] and J. C. Raymond[2]
Received 2008 February 20; accepted 2008 June 4

ABSTRACT

In the wake of the 2003 November 4 coronal mass ejection associated with the largest solar flare of the last sunspot cycle, a current sheet (CS) was observed by the Ultraviolet Coronagraph Spectrometer (UVCS) as a narrow bright feature in the [Fe XVIII] ($10^{6.8}$ K) line. This is the first UV observation in which the CS evolution is followed from its onset. UV spectra provide diagnostics of electron temperature, emission measure, Doppler shift, line width, and size of the CS as function of time. Since the UVCS slit was inside the Mark IV K-coronameter (MK4) field of view, the combination of UV spectra and MK4 white light data provides estimates of the electron density and depth along the line of sight of the CS. The thickness of the CS in the [Fe XVIII] line is far larger than classical or anomalous resistivity would predict, and it might indicate an effective resistivity much larger than anomalous resistivity, such as that due to hyperdiffusion. The broad [Fe XVIII] line profiles in the CS cannot be explained as thermal widths. They result from a combination of bulk motions and turbulence. The Petschek reconnection mechanism and turbulent reconnection may be consistent with the observations.

Subject headings: Sun: activity — Sun: corona — Sun: coronal mass ejections (CMEs) — Sun: UV radiation

1. INTRODUCTION

The largest solar flare of the last sunspot cycle occurred on 2003 November 4. It was the climax of a series of very energetic "Halloween" events, and it was estimated as *GOES* class >X28 (Kiplinger & Garcia 2004). It started at ~19:35 UT, but the *GOES* instruments saturated almost immediately. Kiplinger & Garcia (2004) estimated that the X-ray flare from *GOES* was most probably class X30.6 with a maximum at 19:47 UT. Thus, the flare "produced one of the most intense hard X-ray bursts and the largest soft X-ray burst ever observed" (Kane et al. 2005). The Hα flare occurred near the west limb in active region 10486 at S19°, W83°. Terahertz radio emission was discovered by Kaufmann et al. (2004), who reported very short timescale variability and suggest that this emission arose from electrons considerably more energetic than those responsible for the well-known microwave emission. Kane et al. (2005) used *Ulysses* hard X-ray observations to estimate the peak and total luminosities in energetic electrons, and they found that the total energy liberated in the flare was comparable to the magnetic energy of the active region. The bright post-event arcade (Tripathi et al. 2004) was interpreted as a consequence of the same magnetic reconnection that liberated the coronal mass ejection (CME). Raymond et al. (2007) detected O VI photons from the flare that scattered off O VI ions in the corona, and they determined the flare luminosity at transition region temperatures during the impulsive phase.

Large flares are generally associated with powerful CMEs, and the 2003 November 4 event was no exception. The halo CME detected by LASCO on the *Solar and Heliospheric Observatory* (*SOHO*) reached a speed above 2657 km s^{-1} according to the CDAW CME list (Yashiro et al. 2004), and the kinetic energy estimate is 6×10^{32} erg. These estimates place this CME at the upper end of the CME mass and energy distributions (Vourlidas et al. 2000), but because this was a halo CME, both the mass and kinetic energy may be underestimates.

According to the standard picture for large, long-duration flares, a reconnection CS connects the flare loops to the CME core (e.g., Svestka et al. 1997). The CS is a necessary part of both analytic models (e.g., Lin & Forbes 2000) and numerical simulations (e.g., Riley et al. 2002) of flare/CME events. The CS contributes to the flare energy, allows the CME to escape from the Sun, and creates a helical flux rope that might account for magnetic clouds in interplanetary space (Gosling et al. 2006) or envelop pre-existing magnetic flux ropes (Lin et al. 2004). Recent progress in understanding Hall reconnection (e.g., Bhattacharjee 2004) the intrinsically unsteady, three-dimensional (3D) nature of reconnection (e.g., Cassak et al. 2006), and the role of turbulence (e.g., Lazarian & Vishniac 1999) has been impressive, but there is as yet no agreement on the energy partition of the reconnection process: how much of the magnetic energy dissipated is converted to kinetic energy (directed or turbulent), thermal energy or energetic particles.

In recent years, CS observations have been reported from white light coronagraph observations (Webb et al. 2003), X-ray images (Sui & Holman 2003), radio dynamical spectra (Aurass et al. 2002), extreme-ultraviolet (EUV) images dominated by Fe XII or Fe XXIV (Yokoyama et al. 2001; Innes et al. 2003; Noglik et al. 2005) and coronagraphic UV spectra (Ciaravella et al. 2002; Ko et al. 2003; Lin et al. 2005; Bemporad et al. 2006; Lee et al. 2006). Each of these observations reveals something about the physical conditions in CSs, but most pertain to a single event, and none is complete.

This paper uses UV and white light observations to investigate the CS associated with the 2003 November 4 flare. In this event, a narrow, bright feature appeared in the [Fe XVIII] line shortly after the CME crossed the UVCS slit. Over the course of about 4 hr it faded and became narrower, then remained at a low level for a full day. We derive the temperature, density, physical size, and nonthermal line widths of the CS and compare them with expectations based on Petschek and turbulent reconnection pictures. Sections 2 and 3 describe the white light and UV observations, while the CS analysis is described in § 4. The thickness and

[1] INAF-Osservatorio Astronomico di Palermo, Piazza Parlamento 1, 90134 Palermo, Italy.
[2] Harvard-Smithsonian Center for Astrophysics, 60 Garden Street, Cambridge, MA 02138.

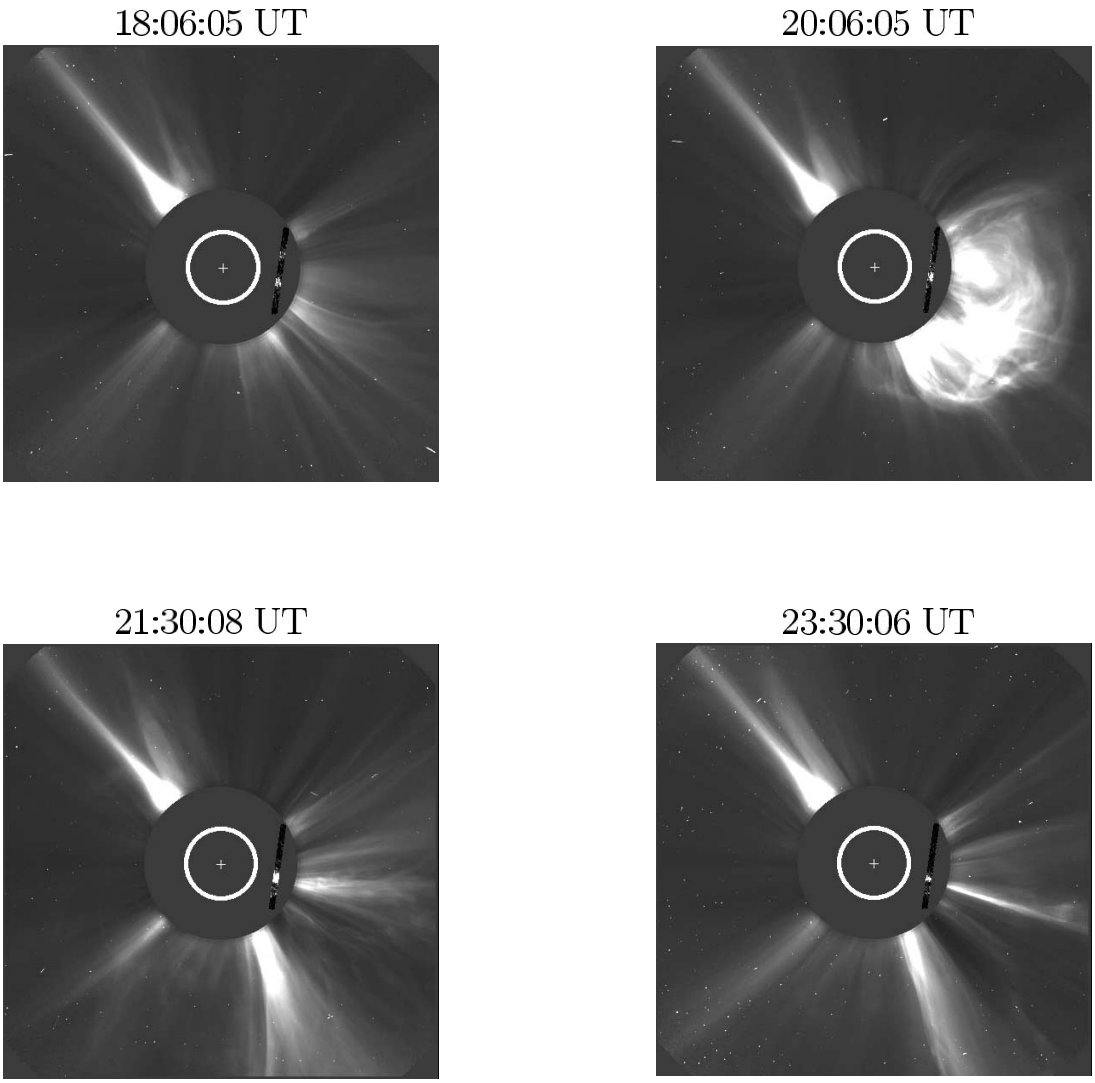

FIG. 1.— LASCO C2 images at four times showing the evolution of the events from the pre-CME corona to the narrow long CS feature. The images shown inside the occulter disk are the intensity distribution of the [Fe XVIII] line along the UVCS slit. The brightest narrow spot is very well aligned with the LASCO CS.

Doppler shift of the CS feature are in § 4.1, the temperature and density in § 4.2, and the line width in § 4.3. We discuss the results in § 5.

2. WHITE LIGHT CORONAGRAPH OBSERVATIONS

We use data from the LASCO C2 coronagraph aboard *SOHO* (Brueckner et al. 1995) and the MK4 at Mauna Loa Solar Observatory (MLSO). The UVCS entrance slit was below the LASCO C2 occulter but within the MK4 field of view. LASCO C2 covers the range from 2.3 to 6.0 $R_\odot$ from disk center with a typical cadence of 24–34 minutes between frames. The halo CME associated with the flare was first detected in LASCO C2 at 19:54:05 UT when the front in the western hemisphere was already at 4 $R_\odot$. The CDAW Web site[3] gives a linear fit to the CME leading edge positions in three C2 frames with a speed of 2657 km s^{-1}. C2 images of the event at 18:06, 20:06, 21:30, and 23:30 UT are shown in Figure 1 along with the intensity distributions of the [Fe XVIII] line observed by UVCS. After the edge of the CME left the C2 field of view, a bright, somewhat diffuse radial structure appeared above the active region at 20:30 UT. Over the next few hours it shifted toward the south and became brighter, narrower, and more stable.

Several plasmoids moved outward along this structure, and others appeared adjacent to the structure and moved parallel to it. Although many plasmoid features were seen flowing outward during the initial phase of the CS, it was difficult to follow them in the white light images. However, we have velocity estimates for three plasmoid features seen flowing outward. The first was detected between the C2 images of 21:30:08 and 21:54:31 UT as a round feature traveling at a projected speed of ~870 km s^{-1}. This feature was seen when the CS appeared very thick in the UVCS data. Later, two plasmoids were detected at in C2 images at 00:30:05 UT and 06:30:05 UT moving outward at speeds of 580 and 480 km s^{-1}, respectively. Assuming a constant speed these two plasmoids should have crossed the UVCS slit around 23:30 on November 4th and 05:40 UT on November 5th. Other plasmoids, which were difficult to follow in sequential images, were also seen between these two.

The Advanced Coronal Observing System (ACOS) data from MLSO consist of the polarized brightness obtained from scans around the solar disk covering the range 1.14–2.86 $R_\odot$ with a resolution of 0.5° in position angle by 5.05″ in the radial direction. Data are available on November 4th for the periods 17:16–18:37

[3] See http://cdaw.gsfc.nasa.gov/CME_list.

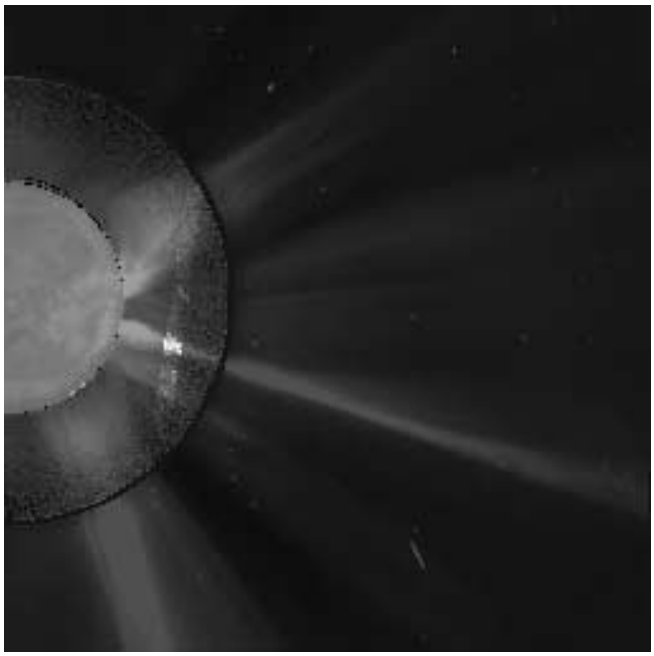

FIG. 2.—Composite image of EIT 195 Å (23:48 UT), MK4 (23:48 UT), LASCO C2 (23:54 UT), and intensity distribution of the [Fe XVIII] line along the UVCS slit.

and 21:04–01:35 UT. Unfortunately, these do not cover the impulsive phase of the flare, but they do cover most of the period when bright [Fe XVIII] was seen with UVCS. For the combined UV/white light analysis, we have extracted the pB values at pixels corresponding to positions along the UVCS slit. The pre-CME scans show a bright feature near P.A. $= 254^\circ$ and a fainter one at P.A. $= 280^\circ$. After the CME, the overall brightness was reduced, and a single bright feature near P.A. $= 253^\circ$ appeared above a smooth background (see last panel in Fig. 5).

This narrow feature seen in LASCO C2 and MK4 connecting the CME with the post flare arcades (see Fig. 2) was very likely the CS predicted by flux-rope model of CMEs. The high-temperature feature observed in the UV spectra at the same location as the LASCO/C2 images in Figure 1 confirms this interpretation (see § 3).

3. UV SPECTRA

The UV spectra of the 2003 November 4 event were taken with UVCS. This instrument aboard *SOHO* measures UV spectra of the solar corona, in the range 945–1270 Å (473–635 Å in the second order), through an entrance slit 42′ long and up to 84″ wide. The slit can be located at any polar angle and at heliocentric distances from 1.5 up to 10 $R_\odot$ (see Kohl et al. 1995 for a more detailed description of the instrument). During the 2003 November 4 CME the UVCS slit was centered at P.A. 262° and heliocentric height 1.66 $R_\odot$, and its width was 28″. Thus the portion of solar corona between P.A. $= 302^\circ$ and 228° was observed through the slit. The spatial binning along the slit was 6 pixels (42″) and the detector was masked into five wavelength ranges 1023–1042, 997–1008, 990–993, 980–967, and 942–964 Å with spectral binning of 0.2, 0.2, 0.3, 0.2, and 0.3 Å, respectively. In this instrument configuration UVCS observed from November 4th at 17:18:40 UT until November 5th at 13:00:03 UT, collecting spectra with 120 s exposure time separated by 10 s readouts. We have used the most recent calibration that includes the degradation of sensitivity since the launch of *SOHO* (Gardner et al. 2002).

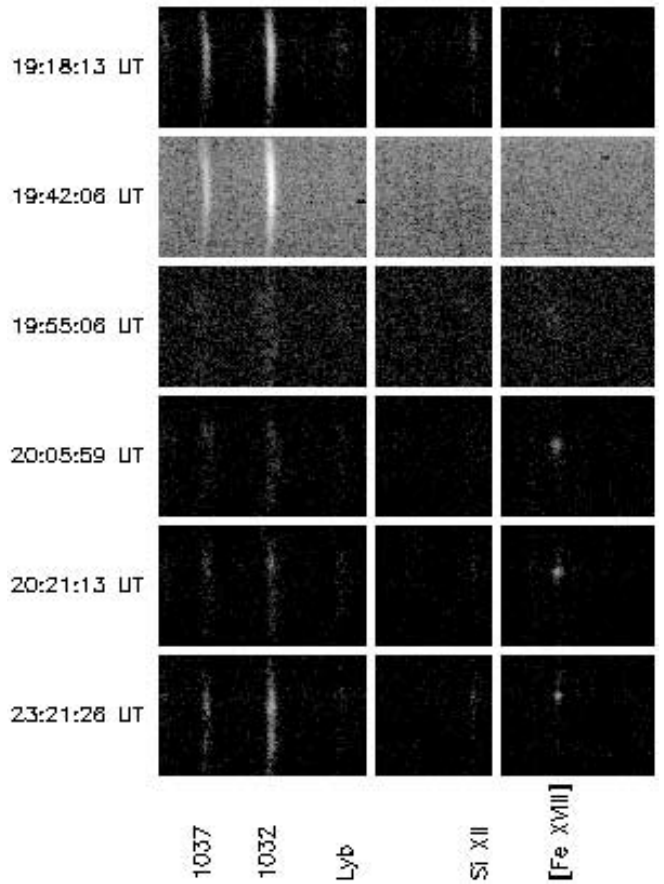

FIG. 3.—UV Spectra for three wavelength ranges, 1023–1042, 997–1008, and 980–967 Å. The main spectral lines are marked in figure. The spectra were taken at 19:18:13, 19:42:06, 19:55:06, 20:05:59, 20:21:13, and 23:21:26 UT and are obtained adding two exposures of 120 s each.

The different phases of the 2003 November 4 CME event are sampled in Figure 3 with three intervals of the UV spectrum at six times. The main spectral lines seen in Figure 3 are the O VI $\lambda\lambda$1032, 1037 doublet, Lyβ, the Si XII $\lambda\lambda$499, 520 doublet, and [Fe XVIII] λ975. The observation started earlier than the CME, and it is important to remark that when UVCS started observing at 17:18:40 UT there was a trailing outflow from an earlier halo CME, detected in LASCO at 12:06:06 UT. Thus the southern bright [Fe XVIII] feature in the preflare spectra at P.A. $= 254^\circ$ was most probably the CS of this earlier CME, while the northern feature around P.A. $= 280^\circ$ appeared in LASCO images as the trail of the ejected structure. The CS from the earlier event was pushed southward by the second CME (at 19:54:05 UT), and it remained in UV spectra as weak feature until the end of the observation. The intensity distributions of the brightest lines of the pre-CME corona are plotted in Figure 4. The main peaks in the [Fe XVIII] lines correspond to the CS at P.A. $= 254^\circ$ and the trailing feature from the earlier CME event. The CS showed a broader range of temperature compared to the northern feature in which the emission was mainly in [Fe XVIII] line.

The second panel from the top in Figure 3 shows the first sign of the underlying activity as a brightening of the O VI lines along the slit due to the flare (Raymond et al. 2007) followed by an increase of the background starting at 19:39:56 UT. The CME front crossed the UVCS slit at 19:42 UT as indicated by the sudden drop in coronal O VI density (Raymond et al. 2007). Five exposures later at 19:52:56 UT, emission from the CME was seen for four exposures as broad and diffuse emission lines of [Fe XVIII] and

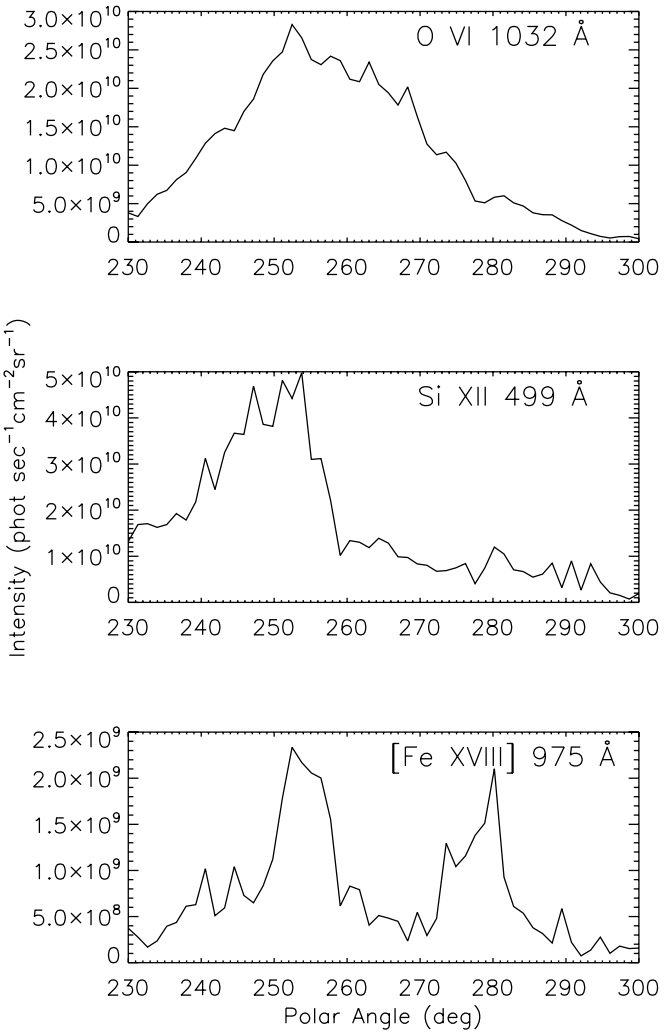

FIG. 4.— Line intensity distributions of the pre-CME corona along the UVCS slit. The position along the slit is given in P.A. The southern feature in the [Fe XVIII] line is most probably the CS from the halo CME detected by LASCO at 12:06:06 UT.

O VI, e.g., third panel from the top. After the bulk of the CME went through the slit, much weaker O VI emission remained, while [Fe XVIII] brightened in a narrow region centered at P.A. = 253°. This feature was detected starting from 19:59:29 UT, about 6 minutes after the first detection of CME, e.g., last three panels in the figure. The emission in the O VI and Si XII lines was severely dimmed as the CME swept out the coronal material (compare the first and fourth spectra in Fig. 3). Later as the postflare loops in the underlying active region started brightening, the emission in these lines increased again. The [Fe XVIII] emission in the wake of the CME was displaced with respect to the peak intensities of O VI and Si XII lines and was well aligned with the bright narrow feature in the LASCO C2 images and the postflare loops seen at lower heights in EIT and *Transition Region and Coronal Explorer* (*TRACE*) images.

4. CS ANALYSIS

Figure 5 shows the images in the [Fe XVIII], O VI λ1032, Si XII λ499, C III λ977 lines and the MLSO MK4 pB along the slit as function of the time. The vertical axis is the polar angle along the slit, and the horizontal axis is the UT time. The vertical bright region in each spectral image is the time of the high background due to the flare, and the emission before that is that of the pre-

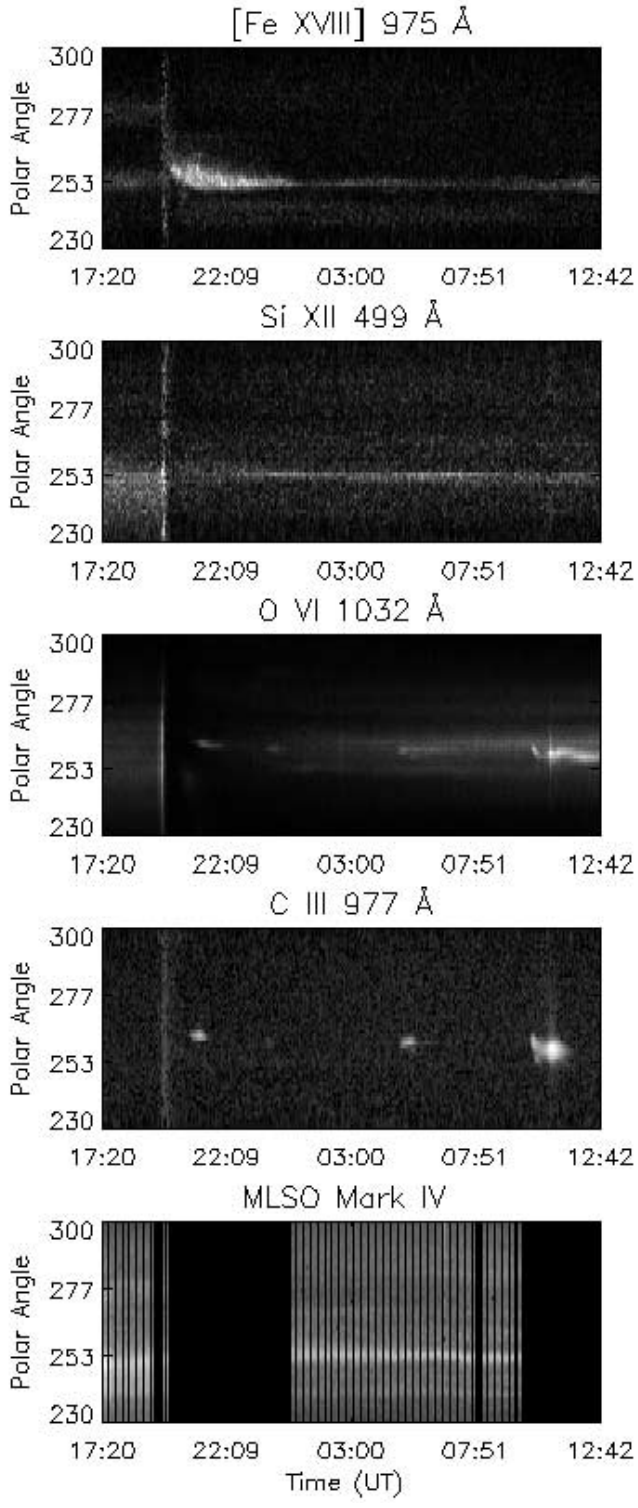

FIG. 5.— Images of [Fe XVIII], Si XII, O VI, C III, and MLSO Mark IV along the slit as function of time. The vertical axis is the position along the slit in polar angle. The vertical bright area in the UV lines corresponds to the high background and passage of the CME. The two horizontal bright regions in [Fe XVIII] emission are from the pre-CME corona (the two main peaks in Fig. 4).

CME corona in the wake of the earlier CME. The long, bright feature centered around P.A. = 253° is the CS. Over a time of about 2.5 hr the peak of the [Fe XVIII] emission moved southward by ~4° and then kept this position until the end of the observation. The spatial extent of the [Fe XVIII] decreased significantly over the first 3 hr (see § 4.1). Similar behavior was observed for

the narrow bright feature in LASCO C2 and MK4 images. The Si XII image also shows the CS starting from $\sim$ 21:40 UT. No similar feature was detected in O VI or C III lines.

The knots seen in C III and O VI lines were cold and narrow ($\sim$126″) transient ejecta, and they were very bright in the lines of Lyβ, N III, Lyγ, and Lyδ as well. We detected three of these events: (1) the first event, at 20:49 UT and P.A. $\sim 265^\circ$, lasted a longer time in O VI than in C III. The peak intensity in C III was 1.5×10^{11} ph s^{-1} cm^{-2} sr^{-1} and in O VI λ1032 it was 3.7×10^{10} ph s^{-1} cm^{-2} sr^{-1}; (2) the second event was detected on November 5th at 04:51 UT and P.A. 262°, first in O VI and then in C III. Like the first event, it lasted longer in O VI. The maximum C III line intensity in this case was 9.7×10^{10} ph s^{-1} cm^{-2} sr^{-1}; (3) the third narrow feature on November 5th at 10:02 UT and P.A. 263° was first detected in O VI lines with a redshift of 400 km s^{-1}. Its Doppler shift decreased to zero in 25 minutes. The feature lasted for more than 60 minutes, and it was probably the same feature seen at 3.1 $R_\odot$ in the later synoptic scan. The feature was also detected in C III, Lyβ, Lyγ, and N III, and the peak intensity of the C III line was 1.5×10^{12} ph s^{-1} cm^{-2} sr^{-1}.

EIT and *TRACE* images showed that these transients all originated from the same location in the active region. In particular, from EIT 195 running difference images these three features corresponded well in P.A. and time to the ejecta from the active region at 20:24 UT on the 4th, 4:12 UT on the 5th, and 10:00 UT on the 5th. These ejecta deviated toward the CS as they, most probably, followed the local magnetic field lines stretched out by the CME. They might have arisen from small reconnection events lower down in the atmosphere as result of rearranging of the magnetic field after the CME eruption. Similar transient events were called "streamer puffs" by Bemporad et al. (2005), who attributed them to the opening of outer loops in the arcade.

In Figure 6 we show the total intensity of the [Fe XVIII] (*top panel*) line in the CS as function of time. This intensity is computed for a portion of 8 bins (336″) along the slit so as to include the initial wider size of the CS. For comparison we plot the Si XII λ499 and O VI λ1032 line intensities (*second and third panel from the top*) in the same portion of the slit as [Fe XVIII] and the O VI λ1032 intensity (*bottom panel*) in the narrow portion (3 bins or 126″) in which the CS was detected in [Fe XVIII] after 22:09 UT in Figure 5. The dashed areas correspond to the exposures in which the CS was not yet detected due to extremely high background from the flare. The two intensity plots for the O VI line show that the emission in this line was mainly due to coronal material along the line of sight (LOS) or to the bright knots detected close to the CS feature. The [Fe XVIII] line intensity increased for 50 minutes, then the emission faded slowly over about 3 hr and remained almost constant for the rest of the observation.

4.1. *Thickness and Doppler Shift*

The image in Figure 5 shows clearly that the [Fe XVIII] emission along the slit became narrower with time. To measure the width of the [Fe XVIII] emission we use the full width half-maximum (FWHM) and the full width (FW) of the feature. These two values are representative of the "bright core" of the emission and of its surrounding region. During the first 3 hr the FWHM changed from 0.2 to 0.1 $R_\odot$ while its FW changed from 0.5 to 0.2 $R_\odot$. Similar values are obtained for the depth along the LOS (see Table 1). The CS geometrical structure was closely related to the postflare loops. AR 10486 in MDI magnetogram images on 2003 November 1 had a longitudinal extent of $\sim$0.2 $R_\odot$ and the postflare loops in EIT 195 images on 2003 November 4 extend along the limb $\sim$0.3 $R_\odot$. These sizes of the active region and post-CME loops agree reasonably well with the apparent thickness and depth along the LOS of the CS. We can estimate the actual thickness of the CS using the 3D schematic in Figure 7. The CS connecting the postflare loops with the CME had extent L, depth along the LOS d, actual thickness w, and apparent thickness l. In the figure, the y-axis is along the LOS, the x-z plane is the plane of the sky (POS), α is the angle between the CS axis and the LOS, β is the angle with the x-z plane or POS. The β angle ranges between 4° and 6° and is given by arctan ($V_{\rm LOS}/V_{\rm POS}$) where $V_{\rm LOS} \leq$ 60 km s^{-1} was the Doppler shift of the [Fe XVIII] line. The speed on the POS, $V_{\rm POS}$, varied between 870 and 580 km s^{-1} as estimated from the plasmoid speeds. The CS was also tilted in the POS with respect to the z-axis by an angle of $\sim$9°, as estimated from the difference between the P.A. of the center of the slit (262°) and the P.A. of the [Fe XVIII] feature (253°). In computing the actual thickness of the CS and its angle with the LOS we will neglect these two angles because they are small and will not contribute significantly to the apparent thickness. Thus the apparent and the actual thicknesses of the CS are

$$l = L \cos(90 - \alpha) + w \sin(90 - \alpha), \quad (1)$$

$$w = d \cos(90 - \alpha). \quad (2)$$

For LOS depths of 0.07–0.2 $R_\odot$ (Table 1), an apparent thickness l of 0.2 $R_\odot$ (FW of the [Fe XVIII] line emission) along the slit, and L of 0.3 $R_\odot$ from the extent of the postflare loop structure, α is between 35° and 25° (or 65° and 55° from the POS), and the actual thickness is 0.04–0.08 $R_\odot$. The actual thickness is 2.5–5 times narrower than the apparent thickness.

Along with the long-lasting feature identified as the CS we detected two transient ejecta in [Fe XVIII] at 19:50 UT and 20:23 UT. The first transient at 19:50 UT was redshifted by 280 km s^{-1}, lasted for two exposures, and then disappeared. The strongly redshifted emission could correspond to a feature at the head of the structure that later narrowed and became the CS. In LASCO C2 this feature was first observed at 20:06:05 UT and moved at a speed of 720 km s^{-1}. At this speed it would have crossed the UVCS slit around 19:42 UT. Given the uncertainties in the speed and the possible acceleration, this is consistent with the redshifted [Fe XVIII] feature detected by UVCS. Later between 20:23 and 20:49 UT, a second transient redshifted by $\sim$180 km s^{-1} was detected $\sim$0.5 $R_\odot$ north of the bright feature in [Fe XVIII]. The redshift corresponds to the time when the bright feature in LASCO C2 moved southward and became narrower. This redshifted material was part of an outflow that may or may not be related to the CS. In the remaining spectra the Doppler shift was less than 60 km s^{-1}.

4.2. *Temperature and Density*

The changes in the line emission in the CS indicate a temperature evolution with time. In particular the CS was initially only detected in the [Fe XVIII] ($10^{6.8}$ K) line, but was later detected in Si XII ($10^{6.3}$ K) and [Ca XIV] ($10^{6.5}$ K) lines as well. Still later, the CS became faint, and we average over groups of exposures to obtain an adequate signal-to-noise ratio. We use the [Fe XVIII] to Si XII line ratio to estimate the temperature of the CS. The line emissivities are taken from CHIANTI version 5 with solar photospheric abundances (Dere et al. 1997; Landi et al. 2006). Coronal abundances would yield the same temperatures. The fourth column in Table 1 shows the temperature for seven time intervals starting from the pre-CME corona. The temperature increased in the CS and reached a maximum value of $10^{6.9}$ K when the emission in [Fe XVIII] was brightest, then decreased to values of $10^{6.62}$ K, similar to the CS of the earlier CME. The second and

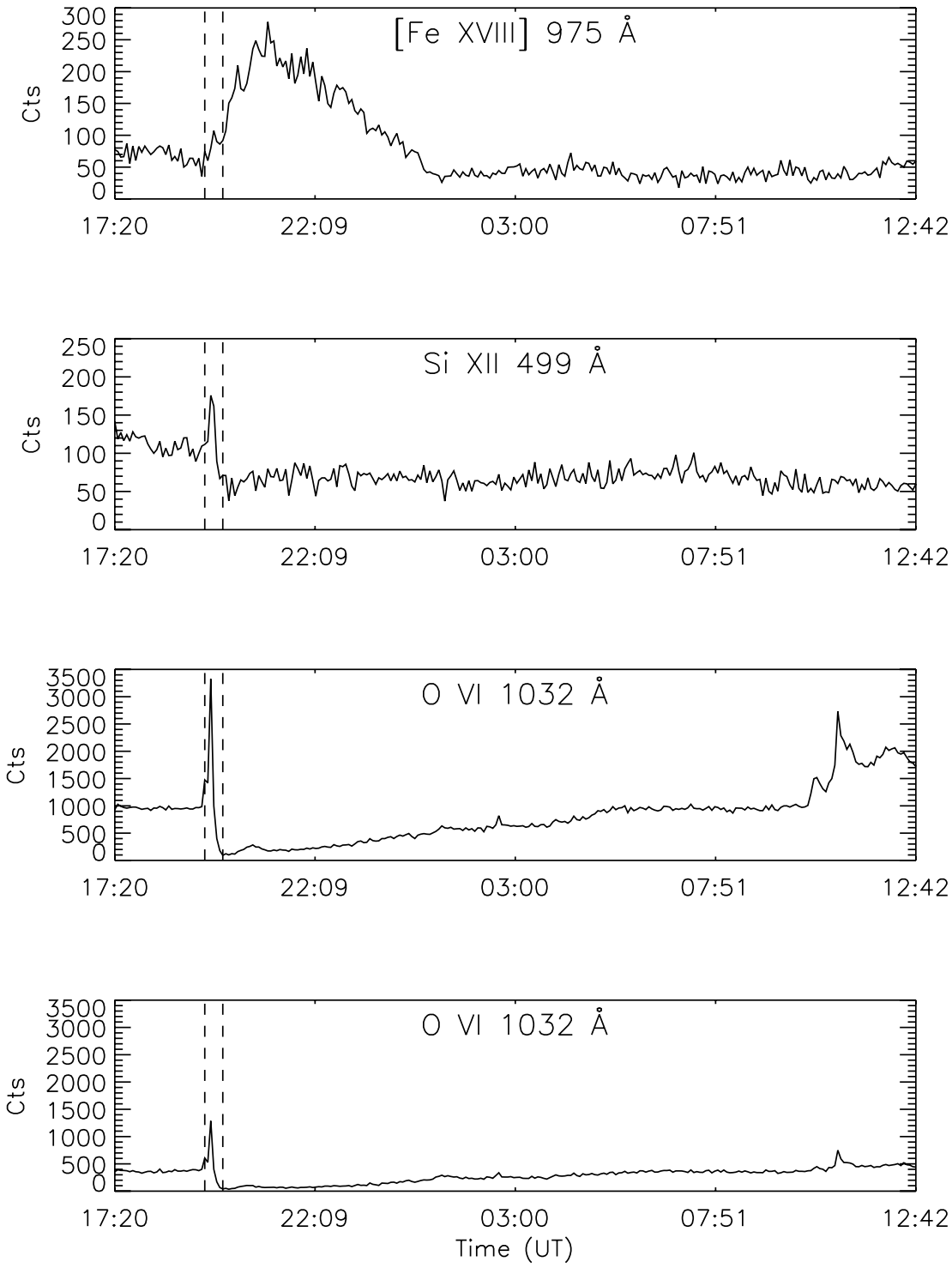

FIG. 6.—[Fe XVIII], Si XII, and O VI total counts inside the CS as function of time. While the first three panels from the top are obtained for a wider portion along the slit, the O VI in the bottom panel is obtained just in the narrow portion the CS is seen in [Fe XVIII] later in the observation. The vertical dashed lines mark the time range when the high background and the passage of CME were detected.

third interval have somewhat larger uncertainties because the CS was very faint in the Si XII line. Given the temperatures, the [Fe XVIII] line intensities were used to determine the emission measure at selected times. The emission measures would be smaller by a factor of 3–4 had we used a coronal abundance set. Values are listed in Table 1.

Electron column densities, N_e, have been obtained from the MLSO Mk4 pB images under the assumption that the gas is in the POS, which is a reasonable assumption for the CS. The ratio of the emission measure, obtained from the [Fe XVIII] intensity, to N_e is the electron density, $n_e = \mathrm{EM}/N_e$. Given n_e, the depth along the LOS is given by $d = N_e/n_e$. In Figure 8 the emission measures, column densities, and densities along the UVCS slit are plotted for the four intervals. The curves of emission measure in the figure are offset by multiples of 2.5×10^{25}, those of column densities by multiples of 4×10^{17}, and the densities by multiples of 4×10^{7}. The peaks at P.A. $= 253^{\circ}$ correspond to the CS.

TABLE 1
CS Parameters

Time (UT)	P.A. (deg)	I_{974}[a] (LU)	I_{499}[a] (LU)	log T (K)	EM (10^{25} cm^{-5})	N_e (10^{17} cm^{-2})	n_e (10^7 cm^{-3})	Depth ($R_\odot$)
17:20–19:09.....	251.6–261.9	1.39	11.0	6.61	2.4	...	...	...
20:27–21:00.....	251.6–261.9	5.13	6.83	6.81	3.1	...	...	...
21:06–21:28.....	251.6–258.9	6.44	6.59	6.90	4.4	4.5	9.8	0.07
22:03–22:35.....	251.6–257.5	5.74	6.95	6.79	3.4	4.9	7.0	0.10
23:19–00:02.....	251.6–256.0	4.06	9.95	6.72	3.4	5.0	6.8	0.11
00:42–01:38.....	251.6–254.5	1.46	9.61	6.62	2.4	5.9	4.1[b]	0.21[b]
03:29–04:57.....	250.2–257.5	1.10	7.72	6.62	1.8	...	...	...

[a] Line Units = ph cm^{-2} s^{-1} sr^{-1}.
[b] Uncertain background subtraction.

It is also worthwhile to consider the total amount of plasma in the CS. Using the ACOS MLSO column densities, N_e, and the apparent thickness in the white light images, h, of the CS in the POS, we plot in Figure 9 $n_e A = N_e h$, where A is the cross-sectional area of the CS. The flux of material along the CS is $n_e A v$, so for constant velocity v (as expected if v is approximately the Alfvén speed), conservation of mass implies that $n_e A$ will be constant at heights above the main reconnection region. Figure 9 shows that $n_e A$ is constant above about 2 $R_\odot$.

4.3. *Line Width*

A Gaussian fit to the line profile is used to compute the FWHM of the [Fe XVIII] line at different times during the observations. The FWHM of the line is corrected for the instrument profile width, 0.32 Å or 100 km s^{-1}, which takes into account the optical distortion, the slit width, and the spectral binning used in the observation. We compute [Fe XVIII] line widths for 23 different time intervals starting from the pre-CME spectra. To improve the statistics of the line profiles we combine several exposures depending on the time interval. In Figure 10 we show the line width values in km s^{-1} as a function of the time. By comparison with Figure 6, the first value corresponds to pre-CME emission, then the remaining values sample the rising, the decaying, and the "quasi" stable phases of the [Fe XVIII] in the CS. The [Fe XVIII] line width shows its maximum value (~380 km s^{-1}) just after the high background due to the flare when the extent on the POS was also large. The other high values (>180 km s^{-1}) could correspond to the passage of the plasmoids along the CS as observed in LASCO (see § 2). The thermal widths of the [Fe XVIII] line corresponding to the seven intervals in Table 1 are shown in Figure 10 by the triangles.

Thus the [Fe XVIII] line width shows a strong nonthermal component during the entire observation. In the pre-CME corona (actually the CS of an earlier CME), it is ~100 km s^{-1}, which is much smaller than the value of ~380 km s^{-1} just after the CME passage or than the values observed during the passage of plasmoid features along the CS. These results suggest that turbulent broadening of the line may be present in the CS, although the LOS component of a systematic bulk flow could also account for the line width if the emitting region is fan shaped. Another possibility is that for the first two values in Figure 10 we detected the bottom

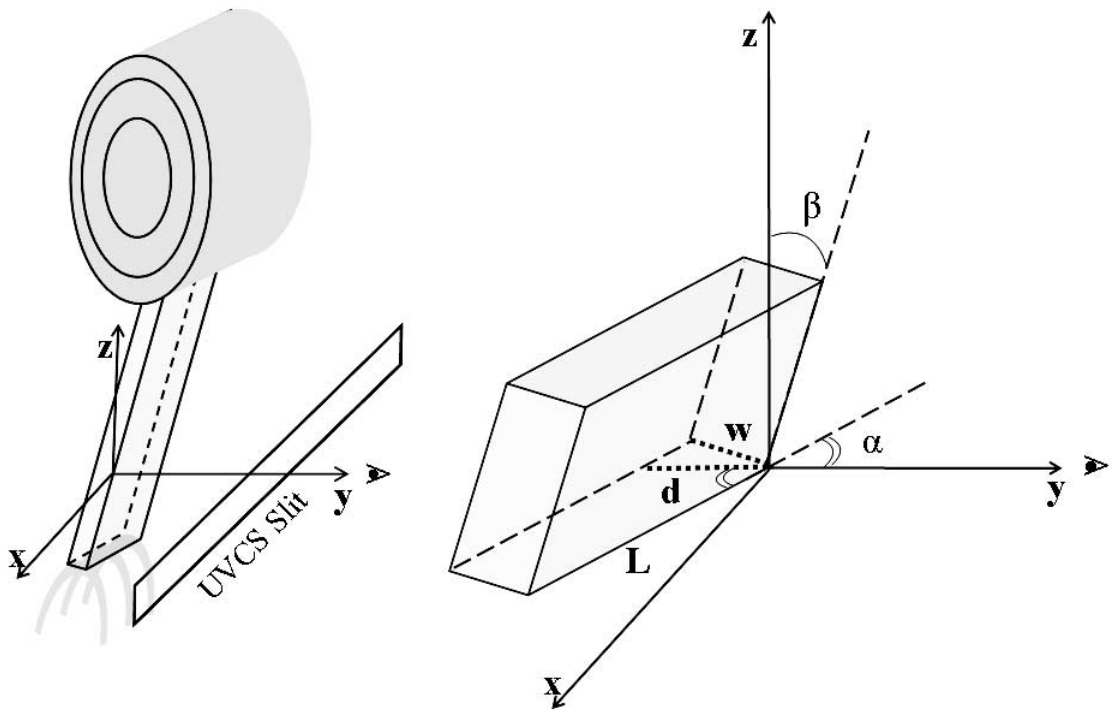

FIG. 7.—Schematic of the CS connecting the postflare loop with the CME as observed through the UVCS slit, left side. On the right side is drawn an enlargement of the CS and its position with respect to an *xyz* coordinate system. The symbols indicate the CS actual extent, L, the actual thickness, w, the depth along the LOS, d, the angle with the plane x-z, β, and the angle with the LOS direction, α.

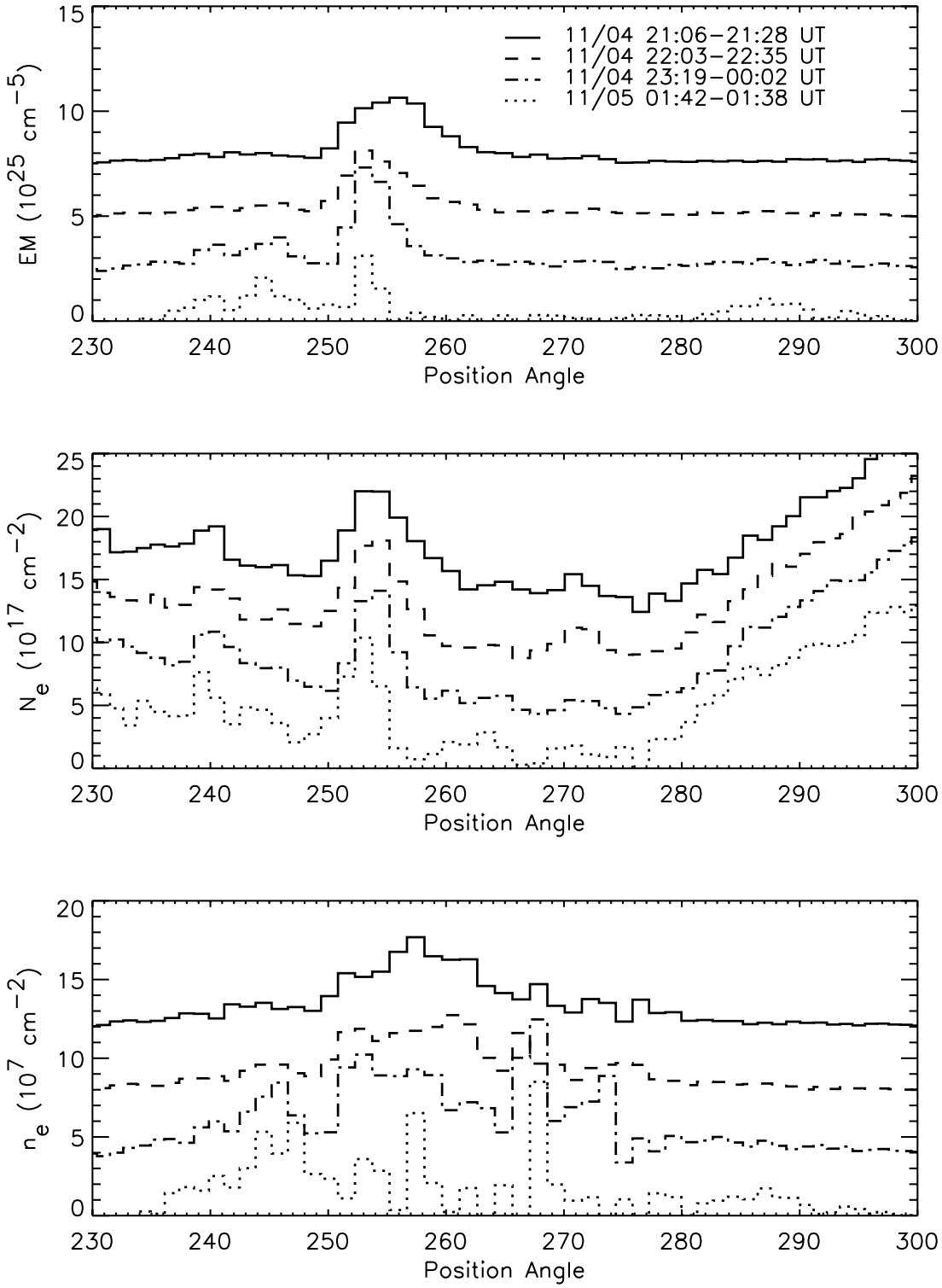

FIG. 8.—Emission measure, column density, and density of the CS for four intervals as shown in figure. The curves have been offset from the top by multiples of 2.5×10^{25}, 4×10^{17}, and 4×10^{7}, respectively, for clarity.

part of the flux rope close to the CS. In this region where the upward reconnection outflow collides with the flux rope, shocks are formed and the flow is deflected away from the vertical direction (Shiota et al. 2005).

5. DISCUSSION

It is important remark that the 2003 November 4 event is, so far, the only CME in which the CS has been detected in UV spectra from its onset. Three of the previous five published events (Ciaravella et al. 2002; Ko et al. 2003; Bemporad et al. 2006) were not detected at the onset of the CS because the observations started long after the CME. The other two (Lin et al. 2005; Lee et al. 2006) were only observed for a few exposures.

The 2003 November 4 CS was characterized in the UV by a bright narrow feature in the high-temperature [Fe XVIII] line that was well aligned with the narrow long feature seen in the

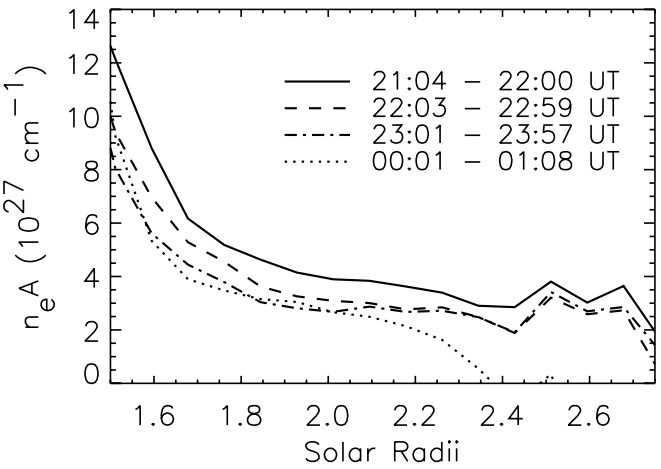

FIG. 9.—Electron density times the cross-sectional area, $n_e A$, of the CS observed in ACOS/MLSO as function of the heliocentric distance at different times.

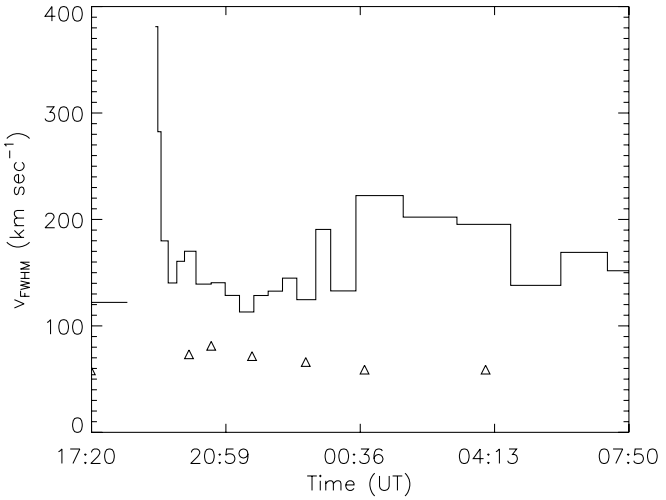

FIG. 10.—[Fe XVIII] line width as function of time. In the figure, the middle times of the selected intervals are shown. The triangles are the [Fe XVIII] thermal widths.

LASCO C2 and MK4 white light images. UV spectra provide diagnostics of temperature, emission measure, Doppler shift, line width, and size of the CS as functions of time. The simultaneous detection of the CS feature in UV spectra and white light images is also unusual. Only two events, 2003 November 4 and 2002 January 8 (Ko et al. 2003), among those published so far have identifiable raylike features in LASCO images of the CME aligned with the [Fe XVIII] feature in UV spectra. In the 2003 November 4 event, the UVCS slit was below the LASCO occulter but inside the MSLO field of view. We were able for the first time to use the combination of the emission measure from UV spectra and the column density from MLSO to estimate the electron density and depth along the LOS of the CS. The results of our analysis can be summarized as follows.

1. The apparent thickness of the CS, measured as FWHM (FW) of its extent along the UVCS slit, was 0.2 (0.5) $R_\odot$ at the early stages, then narrowed to 0.1 (0.2) $R_\odot$ and it kept this value for more then 10 hr. Similar apparent thicknesses have been detected in other events observed by UVCS (Ciaravella et al. 2002; Ko et al. 2003). The depth of the CS as obtained from the combination of UV and MLSO pBs ranges between 0.07 and 0.1 $R_\odot$. The actual thickness was computed and ranges between 0.04 and 0.08 $R_\odot$ [$(3–6)\times10^9$ cm], about 2.5–5 times smaller than the observed FW of the [Fe XVIII] emission along the UVCS slit.

2. Aside from two initial transient features detected in [Fe XVIII] emission, the Doppler shift of the CS was $\leq$60 km s^{-1}, implying that the CS was very close to the POS.

3. The temperature in the CS decreases with time from 8×10^6 to 4×10^6 K. A similar trend in the CS temperature was seen during the 2.5 day observation of the 2002 November 26 CS (Bemporad et al. 2006).

4. The electron density ranges between 7×10^7 and 10×10^7 cm^{-3}, higher than the typical coronal values at the same height. Similar values have been estimated in the CS observed by Bemporad et al. (2006), but they were based on an assumed CS thickness. Using the density and temperature in Table 1, a constraint on the Alfvén speed outside the CS can be estimated by imposing the balance between the CS internal gas pressure and the external magnetic pressure. We obtain, for the time 21:06–21:28 UT, a magnetic field of $\sim$2.2 G. Assuming a factor of 2.5 compression by the slow mode shock in the Petschek picture (Vršnak & Skender 2005), the external density is about 3×10^7 cm^{-3}, and the Alfvén speed is $\sim$800 km s^{-1}. This value agrees with the plasmoid speed along the CS early in the observation.

5. The [Fe XVIII] line widths in the CS are not thermal. They are very broad in the early stages (FWHM = 380 km s^{-1}) and between 50 and 200 km s^{-1} during most of the observation. Such broad line profiles have not been detected in the previously published UVCS observations of CS.

The results just outlined from the 2003 November 4 CS analysis allow us to address in the following a few key questions on CS physics.

5.1. *Reconnection Region*

One important question about the region observed by UVCS in this CS is whether reconnection is occurring at the height of the UVCS slit, or whether the reconnection occurs at an X point at lower altitudes and UVCS sees only the outflowing plasma. If the reconnection outflow has the Alfvén speed of the region near the reconnection site and remains fairly constant, then conservation of mass implies that the density times the cross-sectional area, $n_e A$, will also be constant in regions where reconnection does not occur. From the MLSO white light data, $n_e A$, as shown in Figure 9, is constant above about 1.9 $R_\odot$, but it is still changing in the region of the UVCS slit. This indicates that UVCS is indeed observing the reconnection region, at least until 00:00 UT.

5.2. *CS Thickness*

One major feature of these observations is the apparent thickness of the CS, similar to values reported before (Ko et al. 2003; Ciaravella et al. 2002). However, in these previous cases there was an open possibility that the CS was a very thin sheet viewed almost edge-on. In that case the apparent thickness could have a major contribution from the projection of its depth along the LOS. In the case of the 2003 November 4 CS described in this paper the combination of UVCS spectra and MLSO white light data shows that the projection effect is small. The depth along the LOS is comparable to the apparent thickness on the POS of the [Fe XVIII] emission along the UVCS slit. The hypothesis of a thin sheet would require a very high density to account for the computed emission measure, but the implied column density would be smaller than that obtained from MLSO pB. The actual thickness of the CS as estimated in § 4.1 varies between 0.04 and 0.08 $R_\odot$ and confirms that the LOS depth is only few times larger.

The actual thickness we observed in 2003 November 4, as well as in previous CS, is far larger than the expected thickness of the classical CS diffusion layer, $\leq$100 m for classical resistivity and tens of kilometers for anomalous resistivity. Thus the observed region must be either the region compressed between slow mode shocks in the Petschek mechanism, or it could indicate an effective resistivity much larger than anomalous resistivity, such as that due to hyperdiffusion (Bhattacharjee & Yuan 1995; Lin et al. 2007; van Ballegooijen & Cranmer 2008).

5.3. *Nonthermal Velocities*

Another important result of the observations is the large nonthermal [Fe XVIII] line width which at the early stage of the CS is as high as 380 km s^{-1} and later ranges between 50 and 200 km s^{-1}. Such wide line profiles must result from either bulk flows or turbulence. Candidate bulk flows would be the inflow into the CS or a diverging flow along the CS.

The inflow speed inside the CS can be roughly estimated from the outflow speed of the plasmoid-like features, the ratio of inflow to outflow speeds (Alfvén Mach number) and the compression in the CS. The plasmoid speeds were $\sim$720–870 km s^{-1} during the early stages, and later they declined to values between 580 and 480 km s^{-1}. The Alfvén Mach number should be around 0.05 both to satisfy flare luminosity requirements and on the basis of the observations of Lin et al. (2005). Thus the inflow speed just outside the CS is around 30–50 km s^{-1}. The inflow inside the CS is further diminished, because the compression that makes the CS visible also slows the inflow. For a conservative compression factor of 2.5, the inflow speed is probably about 15–25 km s^{-1}, and the LOS component is a fraction of that. Thus the inflow speed does not contribute significantly to the line width.

The second bulk flow possibility is flow along a fan-shaped CS if the fan is seen edge-on. The FWHM of the [Fe XVIII] line will be the sine of the opening angle times the flow speed. Taking a speed of 870 km s^{-1} at the early stage when the FWHM of the line was 380 km s^{-1} the opening angle of the fan would be 25°, which will give a depth along the LOS of 0.76 $R_\odot$, or 5.3×10^{10} cm. This is a somewhat large value compared to the 0.2 $R_\odot$ longitudinal size of the active region and the value we compute in Table 1. An alternative possibility for such a wide profile is suggested by the Shiota et al. (2005) model, in which a shock is created by the collision of the upward reconnection outflow with the bottom of the flux rope. This hypothesis is also supported by the large spatial extent of the [Fe XVIII] emission along the UVCS slit, which suggests that we initially observed the bottom of the flux rope. The thickness narrowed with time to the "quasi" stable value. During this phase we can evaluate the depth along the LOS by using the plasmoid outflow speed of $\sim$580 km s^{-1} and the FWHM of the [Fe XVIII] line of 50–200 km s^{-1}. Thus, the opening angle of the fan would have to be 5°–20°, or $(1.0-4.2) \times 10^{10}$ cm in depth. These values are not implausible, but they are not supported by the depth along the LOS that was derived from the observations.

If the line widths are not the result of bulk flows, they may indicate the presence of turbulence inside the CS. Lazarian & Vishniac (1999) present a model for a thick, turbulent CS, in which turbulent motions create small regions of intense field gradients and reconnection occurs in many small layers spread throughout the larger region. This picture is in harmony with some of the models for particle acceleration in flares, where particles encounter many small regions of strong electric field (Turkmani et al. 2006). Lazarian & Vishniac estimate the CS thickness as related to the turbulent speed,

$$w \simeq (H\Delta l)^{1/2}\left(\frac{v}{V_A}\right)^2, \quad (3)$$

for $H > \Delta l$, where H is the height (or length) of the CS, Δl is the scale of the turbulence (assumed here to be smaller than H), v is the turbulent speed and V_A is the Alfvén speed. If we take $v/V_A = 0.1$, $H/\Delta l = 1$, and $H \simeq 0.5\ R_\odot$, the predicted thickness is $\leq 4 \times 10^8$ cm (0.006 $R_\odot$). Although turbulence cannot account for the actual thickness of the 2003 November 4 CS, at least according to the simple estimate of Lazarian and Vishniac, it can contribute significantly to broaden the CS. There is some apparent correlation between the CS thickness and the nonthermal line width during the first few hours, but later on there is no correlation; the CS thickness stays fairly constant while the line width varies, most probably due to the outflow of plasmoids along the CS. There is no apparent correlation between the CME height, which should be related to H, and the CS thickness, but that might indicate a limit to the turbulence scale.

An alternative to the turbulent CS would be Petschek reconnection, where the plasma seen in [Fe XVIII] has been compressed and heated by the slow mode shocks. If the plasma β is small, and if the slow mode shocks strongly reduce the magnetic field, then the compression ratio r approaches 2.5 (e.g., Vršnak & Skender 2005). Conservation of mass requires that $Hv_{in}r = wv_{out}$. If we again take $M_A = v_{in}/v_{out} = 0.05$ and $H = 0.5\ R_\odot$, then $w = 0.06\ R_\odot$. This value is within the computed range of the actual thickness, and Petschek reconnection could explain the CS width. However, this mechanism does not obviously produce strong turbulence. If the Petschek model holds, then the [Fe XVIII] line widths must be attributed to bulk motions.

We can conclude that the large values of the CS thickness and line width in the hot line of [Fe XVIII] cannot be explained as consequences of projection effects or bulk speed. Although the Petschek reconnection mechanism appears to be a plausible explanation for the CS thickness, it does not obviously explain the nonthermal line width of [Fe XVIII], and turbulence, as proposed by Lazarian & Vishniac (1999), may also play an important role in the CS.

This work was supported in part by NASA grant NNG06GG78G to the Smithsonian Astrophysical Observatory. A. C. acknowledges support from Italian Space Agency (ASI) under contract I/015/07/0. The authors thank ISSI (International Space Science Institute, Bern) for the hospitality provided to the members of the team on the "Role of Current Sheets in Solar Eruptive Events" where many of the ideas presented in this work have been discussed. This work used data from the Mauna Loa Solar Observatory operated by HAO and the CHIANTI database. CHIANTI is a collaborative project involving the NRL (USA), RAL (UK), MSSL (UK), the Universities of Florence (Italy) and Cambridge (UK), and George Mason University (USA). We thank Y.-K. Ko for comments that improved the clarity of the paper.

REFERENCES

Aurass, H., Vršnak, B., & Mann, G. 2002, A&A, 384, 273
Bemporad, A., Poletto, G., Suess, S. T., Ko, Y.-K., Schwadron, N. A., Elliott, H. A., & Raymond, J. C. 2006, ApJ, 638, 1110
Bemporad, A., Sterling, A. C., Moore, R. L., & Poletto, G. 2005, ApJ, 635, L189
Bhattacharjee, A. 2004, ARA&A, 42, 365
Bhattacharjee, A., & Yuan, Y. 1995, ApJ, 449, 739
Brueckner, G. E., et al. 1995, Sol. Phys., 162, 357
Cassak, P. A., Drake, J. F., & Shay, M. A. 2006, ApJ, 644, L145

Ciaravella, A., Raymond, J. C., Li, J., Reiser, P., Gardner, L. D., Ko, Y.-K., & Fineschi, S. 2002, ApJ, 575, 1116
Dere, K. P., Landi, E., Mason, H., Monsignori Fossi, B. C., & Young, P. R. 1997, A&AS, 125, 149
Gardner, L. D., et al. 2002, in The Radiometric Calibration of *SOHO*, ed. A. Pauluhn, M. C. E. Huber, & R. von Steiger (Noordwijk: ESA), 161
Gosling, J. T., McComas, D. J., Skong, R. M., & Smith, D. W. 2006, Geophys. Res. Lett., 33, L17102
Innes, D. E., McKenzie, D. E., & Wang, T. 2003, Sol. Phys., 217, 247
Kane, S. R., McTiernan, J. M., & Hurley, K. 2005, A&A, 433, 1133
Kaufmann, P., et al. 2004, ApJ, 603, L121
Kiplinger, A. L., & Garcia, H. A. 2004, BAAS, 36, 739
Ko, Y.-K., Raymond, J. C., Lin, J., Lawrence, G., Li, J., & Fludra, A. 2003, ApJ, 594, 1068
Kohl, J. L., et al. 1995, Sol. Phys., 162, 313
Landi, E., Del Zanna, G., Young, P. R., Dere, K. P., Mason, H. E., & Landini, M. 2006, ApJS, 162, 261
Lazarian, A., & Vishniac, E. T. 1999, ApJ, 517, 700
Lee, J.-Y., Raymond, J. C., Ko, Y.-K., & Kim, K.-S. 2006, ApJ, 651, 566
Lin, J., & Forbes, T. G. 2000, J. Geophys. Res., 105, 2375
Lin, J., Li, J., & Forbes, T. G., Ko, Y.-K., Raymond, J. C., & Vourlidas, A. 2007, ApJ, 658, L123
Lin, J., Ko, Y.-K., Sui, L., Raymond, J. C., Stenborg, G. A., Jiang, Y., Zhao, S., & Mancuso, S. 2005, ApJ, 622, 1251
Lin, J., Raymond, J. C., & van Ballegooijen, A. A. 2004, ApJ, 602, 422
Noglik, J. B., Walsh, R. W., & Ireland, J. 2005, A&A, 441, 353
Raymond, J. C., Holman, G. D., Ciaravella, A., Panasyuk, A., Ko, Y.-K., & Kohl, J. 2007, ApJ, 659, 750
Riley, P., Linker, J. A., & Mikić, Z. 2002, J. Geophys. Res. Space Phys., 107, 1136
Shiota, D., Isobe, H., Chen, P. F., Yamamoto, T. T., Sakajiri, T., & Shibata, K. 2005, ApJ, 634, 663
Sui, L., & Holman, G. D. 2003, ApJ, 596, L251
Svestka, Z., Farnik, F., Hick, P., Hudson, H. S., & Uchida, Y. 1997, Sol. Phys., 176, 443
Tripathi, D., Bothmer, V., & Cremades, H. 2004, A&A, 422, 337
Turkmani, R., Cargill, P. J., Galsgaard, K., Vlahos, L., & Isliker, H. 2006, A&A, 449, 749
van Ballegooijen, A. A., & Cranmer, S. R. 2008, ApJ, 682, 644
Vourlidas, A., Subramanian, P., Dere, K. P., & Howard, R. A. 2000, ApJ, 534, 456
Vršnak, B., & Skender, M. 2005, Sol. Phys., 226, 97
Webb, D. F., Burkepile, J., Forbes, T. G., & Riley, P. 2003, J. Geophys. Res., 108, 1440
Yashiro, S., Gopalswamy, N., Michalek, G., St. Cyr, O. C., Plunkett, S. P., Rich, N. B., & Howard, R. A. 2004, J. Geophys. Res., 109, 07105
Yokoyama, T., Akita, K., Morimoto, T., Inoue, K., & Newmark, J. 2001, ApJ, 546, L69